

Dissolution Kinetics of Stilbite at Various Temperatures under Alkaline Conditions

E. T. Glover*, A. Faanu and J. R. Fianko

National Nuclear Research Institute and Radiation Protection Institute, Ghana Atomic Energy Commission, P. O. Box LG 80, Legon-Accra, Ghana

Corresponding author; E-mail: etglover2002@yahoo.com

Abstract

Experiments measuring the dissolution rates of stilbite ($\text{NaCa}_2[\text{Al}_2\text{Si}_6\text{O}_{20}]\cdot 14\text{H}_2\text{O}$) in pH-buffered solutions were performed in batch reactors at 4, 25, 40 and 60 °C. The pH conditions of the buffer solutions ranged from 8.5 to 12.5. The dissolution rates calculated from silicon concentration of the reacting fluid increased with increasing temperature (4–60 °C) and pH. The dissolution rates ranged from 3.45×10^{-8} (mol cm⁻²s⁻¹) at pH 10.7 and 4°C to 1.93×10^{-6} (mol cm⁻²s⁻¹) at pH 12 and 60°C and were pH dependent. The rate law was established as $R = k(a_{\text{OH}})^n$, where k is the rate constant, a is the activity of the OH species and n the reaction order. The n values obtained were, 0.32 at 4 °C, 0.35 at 25 °C, 0.38 at 40 °C and 0.38 at 60 °C. Activation energy determined using Arrhenius plot was 48.45 kJ/mol at pH 9 and 30.88 kJ/mol at pH 12.

Introduction

The current design concept for geological repository of radioactive waste involves the use of multiple barriers, both geological and engineered, to isolate and contain the radioactive materials in the waste. The high sorption capacity, low permeability and the ability to condition its repository porewaters to a highly alkaline pH makes cementitious material an attractive engineered barrier material in the design of a geological radioactive waste repository (Hodgkinson & Hughes, 1999). The high pH condition lowers the solubility of a number of radionuclides and slows corrosion of the metallic components of the repository.

Saturation of the repository with ground water will occur during the post closure phase of the repository and dissolution of calcium silicate hydrate, the main constituent of cement will generate a high alkaline environment. The hyperalkaline plume (pH 12.5–13) will migrate through the repository

and into the host geology. It will dissolve the host rock especially the aluminosilicate followed by precipitation of calcium aluminosilicate hydrate, a zeolite. Reaction between the minerals in the host rock and alkaline plume will alter the barrier properties of the host geology. Zeolites have higher molar volumes than most primary silicates in host rock (Savage, 1996) but it is not known whether alteration will result in changes in properties. Therefore, mineral/rock interaction must be studied in order to predict the behaviour and stability of the host rock surrounding a cementitious radioactive waste repository. In this paper the dissolution rates of stilbite, a zeolite investigated under alkaline conditions at different temperatures is presented.

Materials and methods

Stilbite

Stilbite ($\text{NaCa}_2[\text{Al}_2\text{Si}_6\text{O}_{20}]\cdot 14\text{H}_2\text{O}$) is a hydrated sodium calcium aluminum silicate

of the zeolite group of minerals. Zeolites are crystalline hydrated aluminosilicate minerals of alkali and alkaline earth metals, having infinite three-dimensional atomic structures. The three dimensional structure is based on an infinitely extending framework of $[\text{SiO}_4]^-$ and $[\text{AlO}_4]^-$ – polyhedral (Fig. 1). These polyhedra are linked by their corners to each other by sharing of oxygen ions to produce an open structural form which has internal cavities in which molecules of various sizes can be trapped (Fig. 2). The structural formula

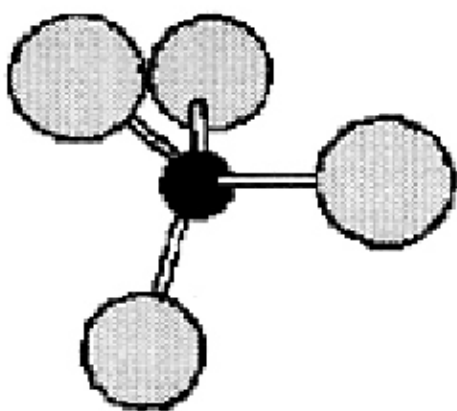


Fig. 1. Three dimensional structure of zeolite

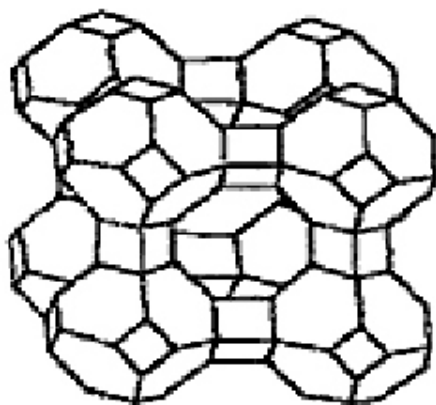
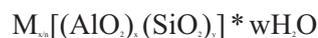


Fig. 2. Structural matrix of a zeolite

of zeolite is based on the crystal unit cell, the smallest unit of structure represented by:



where n is the valence of the cation M , w is the number of water molecules per unit cell, x and y are the total number of tetrahedral per unit cell, and y/x usually has values of 1–5. The charge imbalance of the zeolite framework structure is balanced out by metal cations, which reside in the open channels in coordination with framework oxygens and water molecules both of which have considerable freedom of movement, permitting ion exchange and reversible dehydration without major change of atomic structure. Zeolites have very low specific gravity of 2.0–2.3.

Stellerite ($\text{CaAl}_2\text{Si}_2\text{O}_{10} \cdot 7\text{H}_2\text{O}$) have the same aluminosilicate framework as stilbite but vary in the Si/Al ratio and in concentration and distribution of extra framework cations. In stellerite, due to the absence of Na, only one extraframework site is present whereas in stilbite a small number of Na atoms in a different extra framework site causes the oblique nature of the framework (Quartieri *et al.*, 1987).

Mineral dissolution

Mineral dissolution in aqueous media is a process controlled by reaction at the mineral surface. According to the surface protonation model, used to describe the dissolution process, the surface hydroxyl groups are protonated or deprotonated with variation in pH (Chen & Brantley, 1998). The dissolution rate of minerals is, therefore, dependent on the concentration of the protonated surface sites at $\text{pH} < \text{pH}_{\text{pzc}}$ or the deprotonated site at $\text{pH} > \text{pH}_{\text{pzc}}$, where pH_{pzc} stands for pH of point

of zero net proton charge, or the pH at which the concentration of positively charged surface sites equals the concentration of negatively charged surface sites of the mineral (Chen & Brantley, 2000). The pH dependence of the rate R_i for proton promoted dissolution of mineral is described by an empirical rate law (Wieland *et al.*, 1988):

$$R_i = k [H^+]^n \quad (1)$$

where k is the dissolution rate constant $[H^+]$ is the H⁺ concentration in the aqueous solution and n is a rational exponent which implies a fractional reaction order.

Dissolution rate of minerals increases exponentially with increasing temperature as described by Arrhenius equation

$$k = A \exp(-E/RT) \quad (2)$$

where k is the dissolution rate constant, A is the temperature-independent pre-exponential factor, E is the apparent activation energy of the overall mineral fluid reaction, R is molar gas constant and T is temperature. Activation

energy of the reaction can be obtained from the expression,

$$\ln k = \ln A - (E/RT) \quad (3)$$

as gradient of plot $\ln k$ versus $1/T$.

Sample preparation

Electron microprobe analysis of the stilbite sample (HTL 131), obtained from the British Geological Survey (BGS), Keyworth (U.K), on the basis of framework of 72 oxygen atoms gave the chemical composition shown in Table 1. The sample was crushed, ground in a mortar into fine powder grains and then sieved through a dry nylon sieve to obtain 125–250 μm size fractions. The grains were pre-treated by washing them in alcohol for 1 h, changing the cleaning solution every 5 min, and then dried at 60 °C overnight. The geometric surface area of the grain was calculated assuming all the grains were of uniform size and has a regular spherical geometry. Taking 187.5 μm as the diameter of the spherical

TABLE 1
Electron microprobe analysis of the stilbite (HTL131) sample used in this study

| Oxide | Weight % of oxide | Ion | No of ions on the basis of framework of 72 oxygen |
|--------------------------------|-------------------|------------------|---|
| SiO ₂ | 57.31 | Si | 27.64 |
| Al ₂ O ₃ | 14.22 | Al | 8.08 |
| Fe ₂ O ₃ | - | Fe | - |
| FeO | - | Fe | - |
| MnO | - | Mn | - |
| MgO | - | Mg | - |
| CaO | 8.47 | Ca | 4.40 |
| SrO | - | Sr | - |
| BaO | - | Ba | - |
| Na ₂ O | 1.53 | Na | 1.45 |
| K ₂ O | - | K | - |
| H ₂ O | 18.49 | H ₂ O | 30.12 |
| Total | 100.02 | | |

grain and 2.16 g cm⁻³ the density of stilbite (Breck, 1974) the specific surface area obtained was 0.0148 m²g⁻¹.

Analytical method

Four sets of batch reactor experiments were performed at 4 °C, 25 °C, 40 °C and 60 °C using pH buffer solution with the pH ranging from 8.5 to 12.5 for each temperature. The buffer solutions shown in Table 2 were prepared using the recipes given by Perris and Dempsey, 1974.

the reactors at specified times and acidified with 0.1mL of concentrated HNO₃ for Si analysis. 1 ml of solution from the reactors was also taken during sampling for pH measurement to determine the stability of the buffer solution. The pH was measured immediately the solution had cooled to room temperature. The pH meter electrode was periodically calibrated against standard pH solutions (pH 4 and pH 7) at room temperature. The analytical uncertainty in the pH measurement was ± 0.02. The reaction

TABLE 2
Composition of reacting solution (Perris and Dempsey, 1974)

| pH | Buffer composition A + B + C | Concentration (mol/L) | | |
|------|--|-----------------------|------|--------|
| | | A | B | C |
| 8.5 | Boric acid+Potassium chloride+Sodium hydroxide | 0.05 | 0.05 | 0.010 |
| 9.0 | Boric acid+potassium chloride+Sodium hydroxide | 0.05 | 0.05 | 0.021 |
| 9.5 | Boric acid+Potassium chloride+Sodium hydroxide | 0.05 | 0.05 | 0.0346 |
| 10.7 | Sodium borate + Sodium hydroxide | 0.0125 | | 0.0238 |
| 11 | Sodium chloride + sodium hydroxide | | 0.02 | 0.0015 |
| 12 | Sodium chloride + sodium hydroxide | | 0.02 | 0.0156 |
| 12.5 | Potassium chloride + sodium hydroxide | | 0.05 | 0.0408 |

Each experiment utilised approximately 1g of the prepared sample in 200ml of the pH-buffered solution in plastic batch reactors maintained at the appropriate temperature to an accuracy of ± 1.0 °C. The 4 °C experiment was carried out on a shaker, housed in a room maintained at 4 °C with liquid nitrogen. The 25, 40 and 60 °C batch reactor experiments were carried out in preheated shaking waterbaths at atmospheric pressure. The agitation eliminated temperature gradient within the waterbaths and concentration gradients within the reacting solution in the reactors.

Throughout the experimental period, 10 mL of reacting solution was withdrawn from

bottles were weighed before and after sampling. The headspaces of the reaction bottles were flushed with nitrogen gas after sampling to prevent uptake of CO₂.

Silica analysis was carried out using Mackereth *et al* , 1978 method, which is based on the formation of a blue silicomolybdate complex and the measurement of the colour intensity on a single beam spectrophotometer. Silica standards solutions of 1, 5, 10, 25 and 50 mgL⁻¹ were used for calibration. They were prepared with the buffer solutions (pH 8–12.5) to directly correct for any matrix interference effect from elements in the buffer solutions. Blanks were also prepared

using the buffer solutions. A wavelength of 812 nm was used for the spectrometric reading. The uncertainty in measured Si concentrations was $\pm 3\%$.

Results

Kinetic plots of the total released Si into the buffer solution against time profile ($\Delta t/\Delta V$) are shown in Fig. 3ad. The time profile was measured for accuracy with volume correction made for any leakage or evaporation. The correction involved a differential of experimental run time against volume change. The dissolution rate was determined from the linear regions of the kinetic curves shown in Fig. 3 as far from equilibrium as possible, normalized to the calculated specific surface area of the grain. The dissolution rates are shown in Table 3 and graphically as the logarithm dissolution rate as a function of pH in Fig. 4. The dissolution rates increased with increasing pH and temperature from 3.45×10^{-12} (mol cm⁻²s⁻¹) at pH 10.7 and 4 °C to 1.93×10^{-12} (mol cm⁻²s⁻¹) at pH 12 and 60 °C. The highest rate for the sample was recorded at 60 °C in the pH 12 buffer solution. Dissolution rates were not obtained for the experiments carried out at 4 °C with pH less than 10.5 as the silica concentration was below detection limit.

Activation energy was estimated using the relation

$$\ln(R_1/R_2) = (E/R)(1/T_1 - 1/T_2) \quad (4)$$

where R_1 and R_2 are the dissolution rates at pH of interest and at temperatures T_1 and T_2 , respectively and R is the molar gas constant. The activation energy value decreased from 48.45 kJ/mol at pH 9 to 30.88 kJ/mol at pH 12.

The rate law established by fitting the

logarithm dissolution rates to the pH values was

$$R = k(a_{OH})^n, \quad (5)$$

where k is the rate constant, a is the activity of the OH species and n the reaction order. The n values obtained were, 0.32 at 4 °C, 0.35 at 25 °C, 0.38 at 40 °C and 0.38 at 60 °C. The n values did not compare well with values obtained for stellerite, a zeolite of the stilbite family, which was carried out under similar conditions (Glover & Faanu, 2007). The n values obtained for stellerite were 0.24 at 25 °C, 0.33 at 40 °C and 0.42 at 60 °C. This may be due to the effect of the buffers to keep the pH constant (Chen & Brantley, 1998). Increase in n values with temperature agrees with the surface protonation model that pH dependence of mineral dissolution increases with temperature at $pH < pH_{pzc}$ or $pH > pH_{pzc}$, (Chen & Brantley, 2000).

The variation of n with the reciprocal temperature in Kelvin was also determined (Fig. 5). The linearity of the graph as a function of the inverse of temperature indicates an Arrhenius relation, decreasing linearly with the inverse of temperature. Values of n *in situ* pH of the solutions at 4, 40 and 60 °C were evaluated from the values measured at 25 °C using the computer code EQ3NR version 7.0 (Worley, 1992).

Discussion

The kinetics of the dissolution of the sample was studied by following the release of Si into the buffer solutions. Deprotonation and formation of a precursor complex polarized and weakened the Si-O bonds at the mineral surface, increasing the chance of silicon atoms entering into solution. The initial steep section of the kinetic curves (Fig. 3a-d)

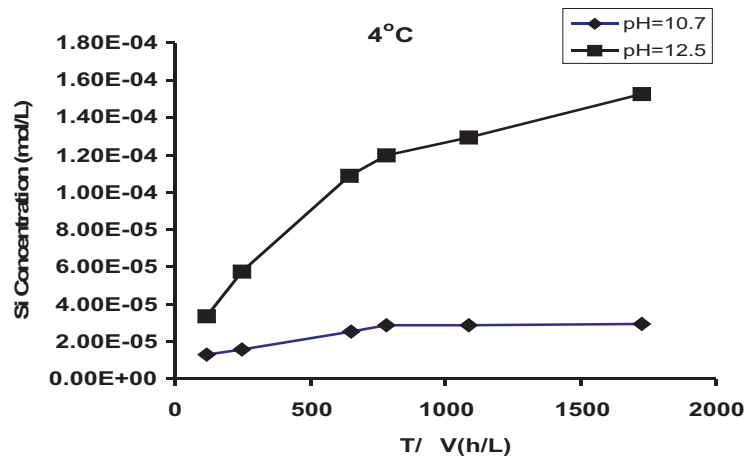


Fig. 3a. Silicon concentration (mol/l) as a function of the time profile (DT/DV) at 4 °C

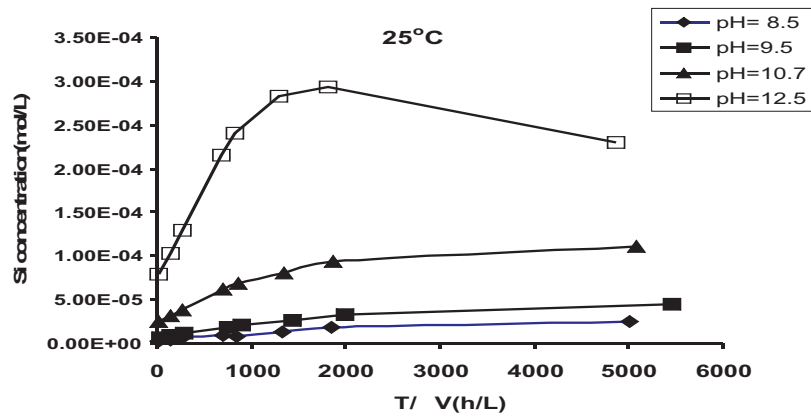


Fig. 3b. Silicon concentration (mol/l) as a function of the time profile (DT/DV) at 25 °C

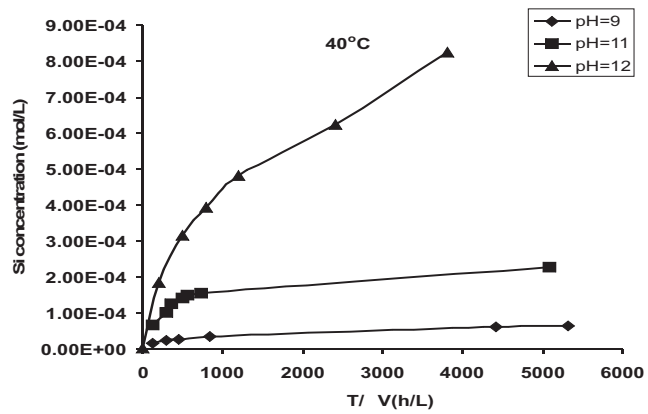


Fig. 3c. Silicon concentration (mol/l) as a function of the time profile (DT/DV) at 40 °C

TABLE 3
 Summary of the dissolution rates of stilbite (HTL 131)

| Temp. °C | pH nominal | Adjusted pH | Si dissolution rate (mol/cm/s) | Log ₁₀ Si dissolution rate (mol/cm/s) |
|----------|------------|-------------|--------------------------------|--|
| 4 | 10.7 | 11.04 | 3.45E-15 | -14.461 |
| 4 | 12.5 | 13.35 | 1.87E-14 | -13.728 |
| 25 | 8.49 | 8.49 | 1.18E-15 | -14.92 |
| 25 | 9.52 | 9.52 | 2.25E-15 | -14.65 |
| 25 | 10.68 | 10.68 | 7.69E-15 | -14.11 |
| 25 | 12.59 | 12.59 | 3.02E-14 | -13.52 |
| 40 | 9 | 8.92 | 7.02E-11 | -10.15 |
| 40 | 11 | 10.65 | 2.98E-10 | -9.53 |
| 40 | 12 | 11.87 | 9.46E-10 | -9.02 |
| 60 | 9 | 8.85 | 2.15E-10 | -9.67 |
| 60 | 11 | 10.14 | 3.98E-10 | -9.40 |
| 60 | 12 | 11.35 | 1.93E-09 | -8.71 |

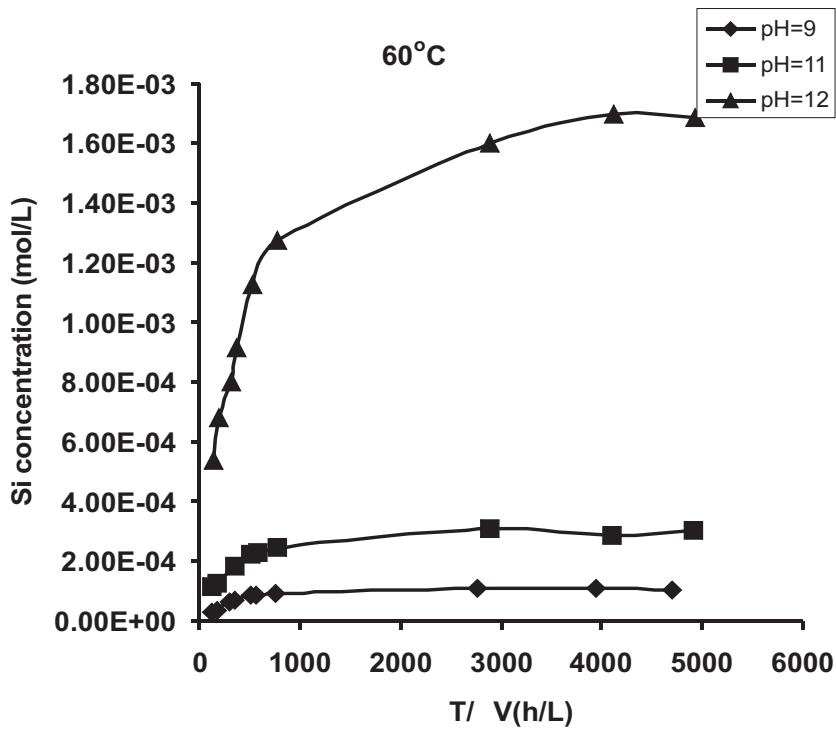


Fig. 3d. Silicon concentration (mol/l) as a function of the time profile (DT/DV) at 60 °C

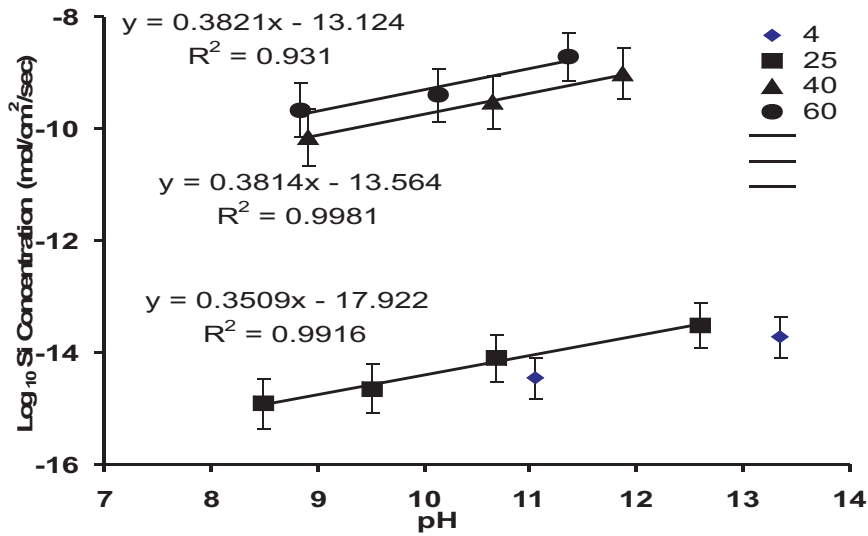


Fig. 4. Rate of stilbite dissolution at variable temperatures and *in situ* pH based on Si release

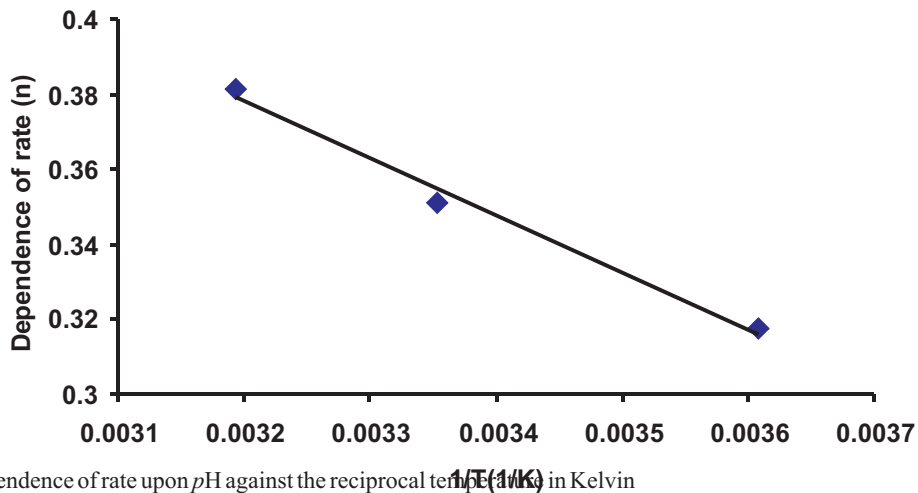


Fig. 5. Dependence of rate upon pH against the reciprocal temperature (1/K) in Kelvin

represented a faster dissolution process due to dissolution of the fine-grained materials from the crushing process, thin edges or corners on the grains (Huertas *et al.*, 1999). The Si concentrations then increased at relatively constant rate before the curve flattened out, approaching steady state equilibrium. Taking samples from the reaction bottles reduced the volume of

reacting solution, and moving the system close towards equilibrium and, thereby, slowing the dissolution rates. Weighing the bottles before and after sampling allowed for volume correction and any leakage or evaporation to be accounted for. The correction involved a differential of experimental run time against volume change ($\Delta t/\Delta V$) as outlined by Bevan *et al.*, 1989.

The effect of the temperature on the dissolution rates is a function of the activation energy E_a , expressed by the Arrhenius equation:

$$k = A e^{-E_a/RT} \quad (6)$$

where E_a represents an apparent activation energy and A is the pre-exponential factor.

Increase in temperature increased the energy in the reacting solution, expressed as an increase in the number of molecules that can potentially exceed the activation energy and form dissolution precursor complexes and, consequently, increase the dissolution rates. Increase in temperature increased the n values slightly (0.33, 0.35, 0.38, and 0.38), but the values were the same within statistical range and, therefore, showed little temperature dependence of the reaction order within the temperature range. The dissolution rate increased with temperature and pH , however,

activation energy decreased with increase in pH . This may be due to data spread.

According to Huertas *et al.*, 2001, activation energy is influenced by the contribution of the enthalpy of adsorption phenomena and may result in the variation in activation energy with pH . There was non-detection of Si release at pH lower than 10.5 at 4 °C because at near neutral pH dissolution rates of minerals containing isolated silica tetrahedra have lower site potentials and have substantially larger temperature dependency (Brady & Walther, 1992).

Compared with other aluminosilicates data found in journals, stilbite had similar dissolution rates with stellerite and illite at 25 °C under alkaline conditions but had higher dissolution rates than quartz, heulandite and anorthite, and lower dissolution rates than kaolinite (Fig. 6).

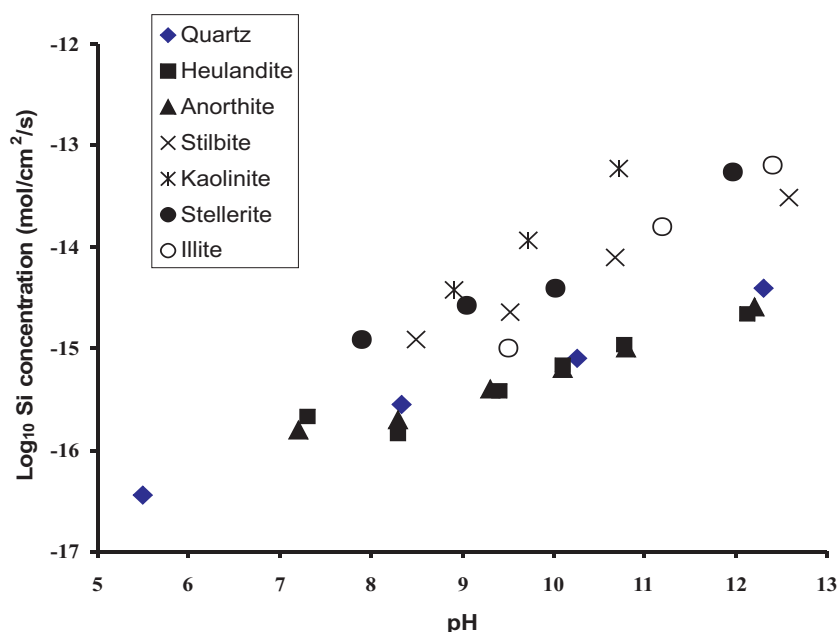


Fig. 6. Comparison of stilbite dissolution rates at 25 °C obtained in this study with dissolution rates of other aluminosilicates available in literature. Data from other studies are: analcime (Savage, 2001), heulandite (Ragnarsdottir, 1993), anorthite (Brady *et al.*, 1989), quartz (Brady and Walther, 1990) and illite (Kohler *et al.*, 2003).

Conclusion

The rate of dissolution increased with temperature and pH from 3.45×10^{-10} (mol cm⁻² s⁻¹) to 1.93×10^{-9} (mol cm⁻² s⁻¹). The dissolution behaviour of stilbite was similar to other aluminosilicates. At constant temperature, increasing the pH increased dissolution rate, whereas at constant pH, dissolution rate increased with temperature. A good linear relationship was established between logarithm dissolution rate and solution pH. The reaction order n increased slightly with increasing temperature. The apparent activation energy was not dependent on pH as it decreased with increase in pH. More experiments using stilbite at different temperatures will give a clearer picture of the variation of rate pH dependency with temperature.

Acknowledgement

The authors would like to thank Dr Liz Bailey of the University of Nottingham as well as Dr Chris Rochelle and Keith Bateman of British Geological Survey, Keyworth, for their immense support, ideas and assistance in carrying out the study. They also thank John Corrie and Darren Hepworth for monitoring the temperature of the waterbaths.

References

- Bevan J.** and **Savage D.** (1989). The effect of organic acids on the dissolution of K-feldspar under conditions relevant to burial diagenesis. *Mineralog. Mag.* **53**: 415–425.
- Brady P.** and **Walther J. V.** (1989). Controls of silicate dissolution rates in neutral and basic pH solutions at 25 °C. *Geochim. Cosmochim. Acta.* **53**: 2823–2830.
- Brady P.** and **Walther, J. V.** (1990). Kinetics of quartz dissolution at low temperatures. *Chem. Geol.* **82**: 253–264.
- Brady P.** and **Walther J. V.** (1992). Surface chemistry and silicate dissolution at elevated temperatures. *Amer. J. Sci.* **292**, pp 639–658.
- Breck D. W.** (1974). *Zeolite Molecular Sieves: Structure, Chemistry, and Use.* John Wiley & Sons, New York, 771 pp.
- Chen Y.** and **Brantley S. L.** (1998). Diopside and anthophyllite dissolution at 25 °C and 90 °C and acid pH. *Chem. Geo.* vol. **147**, pp 233–248.
- Chen Y.** and **Brantley S. L.** (2000). Dissolution of forsteritic olivine at 65 °C and $2 < \text{pH} < 5$. *Chem. Geol.* **165**: 267–281.
- Glover E. T.** and **Faanu A.** (2007). Stellerite dissolution kinetics under hyperalkaline conditions. *J. Appl. Sci Tech.* **12**(1&2): 25–30.
- Hodgkinson E. S.** and **Hughes C. R.** (1999). The mineralogy and geochemistry of cement/rock reactions: high-resolution studies of experimental and analogue materials, *Geo. Soc., Lond.* **157**: 195–211.
- Huertas F. J.** **Chou L.** and **Wollast R.** (1999). Mechanism of Kaolinite Dissolution at Room Temperature and Pressure, Part II: Kinetics Study. *Geochim. Cosmochim. Acta* **63**: 3261–3275.
- Kohler S. J.** **Dufaud F.** and **Oelkers E. H.** (2003). An experimental study of illite dissolution kinetics as a function of pH from 1.4 to 12.2 and temperature from 5 to 50 °C. *Geochim. Cosmochim. Acta* **67**: 3583–3594.
- Mackereth F. J. H.** **Heron J.** and **Talling J. F.** (1978). *Water analysis: some revised methods for limnologists:* Freshwater Biological Association Scientific publication n. 36, Cumbria and Dorset, England, 120 pp.
- Perris D. D.** and **Dempsey B.** (1974). *Buffers for pH and metal ion control.* John Wiley & Sons, New York, 171 pp.
- Quartieri S.** and **Vezzalini G.** (1987). Crystal chemistry of stilbites: structure refinements of one normal and four chemically anomalous samples, *Zeolites.* **7**: 163–170.
- Ragnarsdottir K. V.** (1993). Dissolution kinetics of heulandite at pH 2–12 and 25 °C. *Geochim. Cosmochim. Acta* **57**: 2439–2449.
- Savage D.** (1996). *Zeolites occurrences, stability and behaviour; a contribution to phase III of the Jordan Natural Analogue Project* QuantiSci. DoE Report No DOE/HMIP/RR/95.020.
- Savage D.** **Rochelle C.** **Moore Y.** **Milodowski A.** **Bateman K.** **Bailey D.** and **Mihara M.** (2001).

- Analcime reactions at 25–90 °C in hyperalkaline fluids. *Mineralog. Mag.* **65(5)**: 571–587.
- Wieland E. Wehrli B. and Stumm W.** (1988). The coordination chemistry of weathering: III A generalization on the dissolution rates of minerals. *Geochim. Cosmochim. Acta* **52**: 1969–1981.
- Wolery T. J.** (1992). *EQ3NR, A Computer Program for Geochemical Aqueous Speciation-Solubility Calculations: Theoretical Manual, User's Guide, and Related Documentation* (Version 7.0). Lawrence Livermore National Lab. UCRL-MA-110662-PTIV.